Page Proof Instructions and Queries

Journal Title: The Holocene
Article Number: 609744

Greetings, and thank you for publishing with SAGE. We have prepared this page proof for your review. Please respond to each of the below queries by digitally marking this PDF using Adobe Reader.

Click "Comment" in the upper right corner of Adobe Reader to access the mark-up tools as follows:

For textual edits, please use the "Annotations" tools. Please refrain from using the two tools crossed out below, as data loss can occur when using these tools.

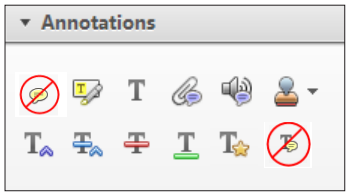

For formatting requests, questions, or other complicated changes, please insert a comment using "Drawing Markups."

Detailed annotation guidelines can be viewed at: http://www.sagepub.com/repository/binaries/pdfs/AnnotationGuidelines.pdf
Adobe Reader can be downloaded (free) at: http://www.adobe.com/products/reader.html.

No.	Query
	Please confirm that all author information, including names, affiliations, sequence, and contact details, is correct.
	Please review the entire document for typographical errors, mathematical errors, and any other necessary corrections; check headings, tables, and figures.
	Please ensure that you have obtained and enclosed all necessary permissions for the reproduction of artworks (e.g. Illustrations, photographs, charts, maps, other visual material, etc.) Not owned by yourself. Please refer to your publishing agreement for further information.
	Please note that this proof represents your final opportunity to review your article prior to publication, so please do send all of your changes now.
	Please confirm that the funding statement is accurate.
1	'Swindles et al. (2011)' is not listed in the references. Please provide reference details or delete the citation.
2	'Maitre (2002)' is not listed in the references. Please provide reference details or delete the citation.
3	'Savov et al. (2009)' is not listed in the references. Please provide reference details or delete the citation.
4	'Thorarinsson (1967, 1976, 1981)' is not listed in the references. Please provide reference details or delete the citation.
5	'Salmi (1948)' is not listed in the references. Please provide reference details or delete the citation.
6	'Rea et al. (2012)' is not listed in the references. Please provide reference details or delete the citation.
7	'Chourpa et al. (2005)' is not listed in the references. Please provide reference details or delete the citation.
8	'Tsai & Philpot (n.d.)' has been changed to 'Tsai and Philpot (1998)' to match the reference list. Please check and confirm.
9	Please note that the citation to Figure 9 in the sentence 'As one can observe in …' has been changed to Figure 7 per context. Please check.
10	'Di Carlo et al. (2010)' is not cited in text. Please indicate where a citation should appear or delete the reference.
11	Please check whether the authors name are correct as given for 'Krucnra and Hnvrr (1994)'.
12	Please check whether the inserted details are correct for 'Tsai and Philpot (1998)'.
13	Please note that Figures 7, 8 and 6 have been renumbered as Figures 6–8, respectively, to maintain sequential order. Please check.

Research paper

The Holocene
1–6

DOI: 10.1177/0959683615609744
hol.sagepub.com
SAGE

Raman spectroscopy for the discrimination of tephras from the Hekla eruptions of 1510 and 1947

Alexander PH Surtees,[1] Graeme T Swindles,[2] Tasnim Munshi,[1] Ivan P Savov,[3] Ian J Scowen[4] and Howell GM Edwards[1]

Abstract

Tephrochronology (the dating of sedimentary sequences using volcanic ash layers) is an important tool for the dating and correlation of sedimentary sequences containing archives and proxies of past environmental change. In addition, tephra layers provide valuable information on the frequency and nature of ash fallout from volcanic activity. Successful tephrochronology is usually reliant on the correct geochemical identification of the tephra which has, until now, been based primarily on the analysis of major element oxide composition of glass shards using electron probe microanalysis (EPMA). However, it is often impossible to differentiate key tephra layers using EPMA alone. For example, the Hekla AD 1947 and 1510 tephras (which are found as visible layers in Iceland and also as 'crypto-tephra' microscopic layers in NW Europe) are currently indistinguishable using EPMA. Therefore, other stratigraphic or chronological information is needed for their reliable identification. Raman spectroscopy is commonly used in chemistry, since vibrational information is specific to the chemical bonds and symmetry of molecules, and can provide a fingerprint by which these can be identified. Here, we demonstrate how Raman spectroscopy can be used for the successful discrimination of mineral species in tephra through the analysis of individual glass shards. In this study, we obtained spectra from minerals within the glass shards – we analysed the microlites and intratelluric mineral phases that can definitely be attributed to the tephra shards and the glass itself. Phenocrysts were not analysed as they could be sourced locally from near-site erosion. Raman spectroscopy can therefore be considered a valuable tool for both proximal and distal tephrochronology because of its non-destructive nature and can be used to discriminate Hekla 1510 from Hekla 1947.

Keywords

discrimination, Hekla 1947, Hekla 1510, Raman, spectroscopy, tephra

Received 12 May 2014; revised manuscript accepted 22 July 2015

Introduction

Distal tephrochronology in NW Europe is a well-established tool for the correlation and dating of sedimentary sequences and palaeoclimate records (Haflidason et al., 2000; Larsen et al., 1999; Swindles et al., 2011).**[AQ: 1]** There have been numerous studies where geochemical correlation of distal tephra deposits with volcanic sources in Iceland was achieved successfully (Hall and Pilcher, 2002). This has primarily been carried out using electron probe microanalysis (EPMA) on the volcanic glasses, always through the analysis of individual shards. However, discrimination based on EPMA alone has some limitations as the glass composition of tephra erupted from same vent or from multiple volcanic sources in any given volcanic cluster may be indistinguishable in major element content. The widely used volcanic rock classification schemes (so called 'TAS diagrams, for total alkalis vs. SiO_2', or the 'K vs. SiO_2' diagram; see Maitre, 2002) are designed on the fact that bulk rock major element compositions of global volcanic rock datasets form clusters (for basalt, andesite, dacite, rhyolite, etc.).**[AQ: 2]** Moreover, the process of basaltic magma evolution and the predictable crystal fractionation of common rock forming minerals (olivine, pyroxenes, feldspars, oxides of Fe and Ti, etc.) can lead to very similar residual glass major element compositions. This is especially true for felsic (dacitic or rhyolitic) eruptions, which always erupt pumice with very low MgO and FeO and very high alkali and SiO_2 contents (Savov et al., 2009).**[AQ: 3]**

Hekla is one of the most active volcanoes in Iceland. It is a stratovolcano located near the rift-transform fault junction in the area where Iceland's Southern and Eastern Seismic Zones meet (Thordarson and Larsen, 2007). Hekla's repeated fissure eruptions result in the formation of a vaulted ridge of about 5 km (*Heklugjá* fissure) that opens along its entire length during major eruptions. All known Hekla eruptions have begun with an explosive phase, followed by a period of more effusive eruptions (Thordarson and Larsen, 2007). After the eruptions in 1693, 1845

[1]School of Chemistry and Forensic Sciences, Faculty of Life Sciences, University of Bradford, UK
[2]School of Geography, University of Leeds, UK
[3]Institute of Geophysics and Tectonics, School of Earth and Environment, University of Leeds, UK
[4]School of Chemistry, University of Lincoln, UK

Corresponding author:
Alexander PH Surtees, School of Chemistry and Forensic Sciences, Faculty of Life Sciences, University of Bradford, Bradford BD1 1DP, UK.
Email: a.p.h.surtees@bradford.ac.uk

Table 1. Glass chemistry data of the tephra from the Hekla eruptions of 1510 and 1947.

Analysis	SiO_2	TiO_2	Al_2O_3	FeO_t	MnO	MgO	CaO	Na_2O	K_2O	Total
Hekla 1510	63.61	1.07	15.56	7.65	0.23	1.19	4.21	4.48	1.83	99.82
Hekla 1510	63.44	1.02	15.24	7.86	0.21	1.34	4.69	4.21	1.77	99.82
Hekla 1510	63.05	0.97	15.44	7.89	0.24	1.39	4.28	4.50	1.69	99.43
Hekla 1510	62.84	1.01	15.03	7.89	0.21	1.36	4.55	4.45	1.76	99.09
Hekla 1510	62.76	0.98	15.25	7.91	0.20	1.37	4.75	4.53	1.74	99.49
Hekla 1510	62.68	0.77	15.01	7.76	0.26	1.32	4.46	4.69	1.78	98.33
Hekla 1510	62.29	0.95	15.17	7.45	0.30	1.25	4.54	4.42	1.71	98.10
Hekla 1510	61.98	0.99	15.18	7.98	0.24	1.34	4.55	4.28	1.77	98.31
Hekla 1510	61.95	0.93	15.13	7.87	0.21	1.26	4.55	4.73	1.74	98.36
Hekla 1510	61.93	0.87	15.19	7.69	0.19	1.16	4.39	3.89	1.75	97.06
Average	62.65	0.96	15.22	7.80	0.23	1.30	4.50	4.42	1.75	98.78
Standard deviation	0.61	0.08	0.17	0.16	0.03	0.08	0.17	0.24	0.04	0.89
Analysis	SiO_2	TiO_2	Al_2O_3	Fe_2O_3	MnO	MgO	CaO	Na_2O	K_2O	Total
Hekla 1947	63.91	1.03	15.12	7.80	0.21	1.25	4.17	4.18	1.66	99.33
Hekla 1947	63.34	0.98	14.96	7.46	0.22	1.23	4.30	4.27	1.75	98.51
Hekla 1947	62.97	0.92	15.34	7.72	0.24	1.25	4.42	4.83	1.88	99.50
Hekla 1947	62.56	1.03	15.13	8.12	0.27	1.36	4.66	4.25	1.71	99.08
Hekla 1947	62.51	0.88	15.30	8.09	0.20	1.14	4.54	4.77	1.65	99.08
Hekla 1947	62.14	0.96	15.02	7.88	0.24	1.18	4.28	3.95	1.73	97.39
Hekla 1947	62.01	0.91	15.28	7.99	0.20	1.32	4.40	4.26	1.77	98.13
Hekla 1947	61.03	0.92	15.11	8.12	0.22	1.31	4.52	4.59	1.66	97.49
Hekla 1947	60.07	1.33	15.13	8.63	0.26	1.73	5.15	2.88	1.61	96.77
Hekla 1947	59.09	1.15	15.19	8.98	0.24	1.71	4.99	4.52	1.69	97.48
Average	61.96	1.01	15.16	8.08	0.23	1.35	4.54	4.25	1.71	98.28
Standard deviation	1.49	0.14	0.12	0.44	0.02	0.21	0.31	0.55	0.08	0.96

Source: Larsen et al. (1999).

and 1947, tephra fallouts were recorded in contemporary written accounts (Thorarinsson, 1981).**[AQ: 4]** Among the most recent eruptions of Hekla, only two have been accompanied by tephra layers (Salmi, 1948; Thordarson and Larsen, 2007).**[AQ: 5]** This is a common problem in tephra studies and is because of the fact that tephra blankets can either disappear (often completely after major erosion because of an associated rainfall event) or are never been deposited at a particular site. During the last 1100 years, Hekla produced 17 widespread silicic tephra layers. All of these tephra layers have been analysed with EPMA, and the dates of these eruptions responsible for producing these tephras have good chronological constraint (Haflidason et al., 2000).

In this paper, we illustrate an alternative tool for analysis of volcanic glass using tephra samples which are nearly identical in composition, tephra erupted from Hekla in 1510 and in 1947. The 1947 Hekla eruption is considered to be of Plinian type (VEI=4) and lasted a full year (29 March 1947 to 21 April 1948). During this event, 0.8 km^3 of lava and 0.21 km^3 of tephra were erupted (Thorarinsson, 1967, 1976). The 1510 eruption of Hekla inevitably has been less well studied, but analysis of contemporary writings suggests that it was a VEI=4 Plinian eruption which produced a tephra blanket that is volumetrically similar to the one after the Hekla 1947 eruption (Sverrisdottir, 2007).

High-quality EPMA data for these tephras are available from both Iceland and Ireland (Tables 1 and 2 and Figure 1). Because of the very small glass shard sizes, there has been no mineral species discrimination based on the standard optical microscopy (e.g. Rea et al., 2012).**[AQ: 6]** This is particularly true for the distal deposits in peats, where often only a few glass shards can be retrieved successfully. In this paper, we demonstrate how Raman spectroscopy can be used to distinguish between microlites within the glass shards from the Hekla eruptions of AD 1510 and 1947 with otherwise indistinguishable major oxide compositions (see Tables 1 and 2). Through this discrimination, we also demonstrate how Raman spectroscopy is able to definitively distinguish between the two tephras for the first time without the aid of optical or other destructive analytical techniques. We also demonstrate how Raman spectroscopy has the potential to offer greater discriminatory power compared with the widely used EPMA analysis approach alone.

Raman spectroscopy is a spectroscopic technique used to study vibrational and rotational modes in a molecular system. It relies on inelastic scattering, or Raman scattering, of monochromatic light, usually from a laser in the visible, near infrared (IR), or near ultraviolet range. The Raman effect occurs when light impinges upon a molecule and interacts with the electron cloud and the bonds of that molecule. For the spontaneous Raman effect, which is a form of scattering, a photon excites the molecule from the ground state to a virtual energy state. When the molecule relaxes, it emits a photon and it returns to a different rotational or vibrational state. The difference in energy between the original state and this new state leads to a shift in the emitted photon's frequency away from the excitation wavelength. The Raman effect, which is a light scattering phenomenon, should not be confused with absorption (as with fluorescence) where the molecule is excited to a discrete (not virtual) energy level.

Raman-active vibrations occur when there is a change in polarizability in the electrons surrounding the atoms. The method is most sensitive to the modes of vibration which are associated with the greatest changes of polarizability, which tend to be symmetrical vibrations. By contrast, IR spectroscopy is most sensitive to asymmetric modes of vibration (which tend to be associated with dipole changes). Raman and IR spectroscopy thus form a complimentary pair of techniques.

Raman spectroscopy is not only confined to the study of low frequency modes of vibration. Provided that the vibrations are

Table 2. Systematic development of Raman settings.

Sample	Exposure time (s)	No. of accumulations	Laser power (%)	Spectral range (cm^{-1})
Goethite	10	10	0.1	100–2000
	10	10	0.5	100–2000
	10	10	1.0	100–2000
	10	10	5.0	100–2000
	20	10	5.0	100–2000
Haematite	10	10	0.1	100–2000
	10	10	0.5	100–2000
	10	10	1.0	100–2000
	10	10	5.0	100–2000
	20	10	5.0	100–2000
Magnetite	10	10	0.1	100–2000
	10	10	0.5	100–2000
	10	10	1.0	100–2000
	10	10	5.0	100–2000
	20	10	5.0	100–2000
	60	10	5.0	100–2000
	20	10	10.0	100–2000

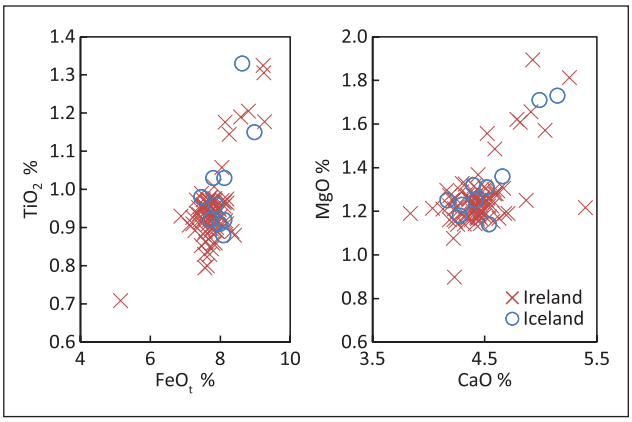

Figure 1. EPMA graphs highlighting the relative percentages of the main elemental oxides of distal (Iceland) and proximal (Iceland) Hekla 1947 (Larsen et al., 1999; Rea et al., 2012).

Raman-active, it can be used to investigate the highest to the lowest frequency vibrations. It is able to identify vibrations between structural groups such as SiO_4 and MgO_6 and, at lower frequencies, vibrations between these structural groups. Because the lengths and angles of the bonds are characteristic of the structural groups and the atoms they contain, so the number and frequency of the vibration are characteristic of these groups also. Because of minerals containing distinctive arrangements of structural groups, their vibrations can be used to identify the motions of atoms within the mineral structure and hence the mineral itself.

Sample preparation and analytical techniques

The tephra glass shards of Hekla 1510 and Hekla 1947, from exposed sections of the deposits in Iceland, were treated with acid (concentrated Sulphuric acid 98% and Nitric acid 68–72%) in order to remove any organic materials but leave, unchanged, the inorganic matter (glass and crystals; see details in Swindles et al., 2010). This particular method is widely used (http://www.tephrabase.org), although two alterations were made to ensure clean surfaces were achieved. These included heating the sample under reflux in order to ensure the mixture was not able to boil dry and to heat with stirring to ensure the complete digestion of organic materials (Edwards et al., 2011). It is essential to ensure the tephra samples are 'clean' and free from any extraneous mineral grains. Any extraneous mineral grains causing contamination of the sample may cause contamination of the resulting spectra and thus prejudice the analysis of the tephra. Powder x-ray diffraction was carried out on both samples pre- and post-treatment to ensure the mineralogy was not altered by utilising this method.

The Raman spectra were obtained using a Renishaw InVia Reflex dispersive spectrometer using the *Reflex* Raman microscope with a diode laser operating at 633 nm with a thermoelectrically cooled charged coupled device (CCD) detector. The instrument is coupled with a Renishaw RE 02 confocal *Leica* microscope with 5×, 20× and 50× objective lenses. The diffraction grating of the instrument provides a spectral range of 3200–100 cm^{-1} with a spectral resolution of 2 cm^{-1}. The instrument was calibrated daily by recording the Raman spectrum of pure silicon (1 accumulation, 10 s exposure time, 100% laser power in static scan mode). When necessary drift corrections were performed to ensure the position of the silicon band was at 520.5 ± 0.1 cm^{-1}. The instrument requires very little in the way of sample preparation; the tephra sample (~0.1 g) was simply spread on a glass slide and placed on the stage in the spectrometer. In total, 50 spectra of each sample were collected over random sampling sites. We analysed the microlites and intratelluric mineral phases that can definitely be attributed to the tephra shards and the glass itself. Phenocrysts were not analysed as they could be sourced locally from near-site erosion.

Spectra were obtained with an accumulation of 10 scans, 10 s exposure time, 1% laser power (approximately 50 mW at source) and 633 nm excitation as these settings had been shown to be the optimum collection parameters. Initial data collected with the Raman spectrometer suggested the presence of three iron oxides: Haematite, Goethite and Magnetite. As a result of these initial spectra, experimental methods were designed to interrogate the iron oxide species found within the glass shards from the Hekla eruptions of AD 1510 and 1947. Experimental parameters had to be carefully and systematically designed (Table 2) as it is well documented that laser power and localised heating can cause these iron oxide species to interconvert (Muralha et al., 2011). In the case of all three iron oxides, experimental parameters were changed in order to produce a 'burn'. These 'burns' were shown by a distinctive colour change on the sample surface (supplementary file 1, available online) as well as a slight change in spectral features (Figure 2). The settings used to cause these 'burns' became the upper limits of the Raman collection parameters.

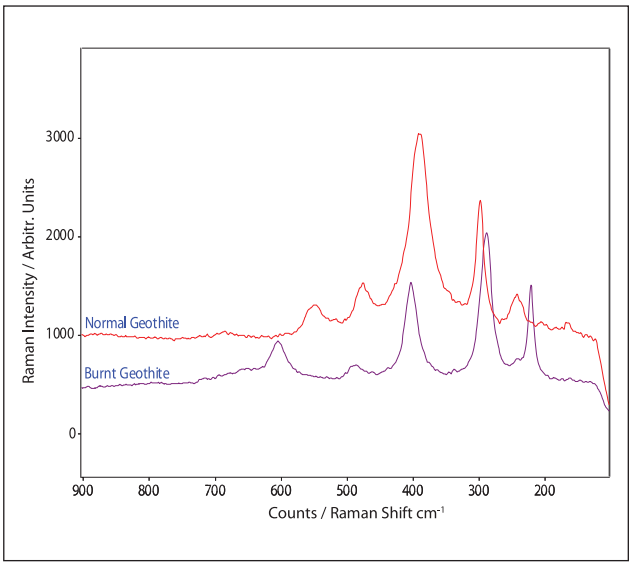

Figure 2. Overlaid spectra showing the spectral changes between normal and burnt goethite. These changes were deliberately caused by increasing the laser power in order to determine the maximum laser power that could be used in the tephra analysis without causing mineralogical changes.

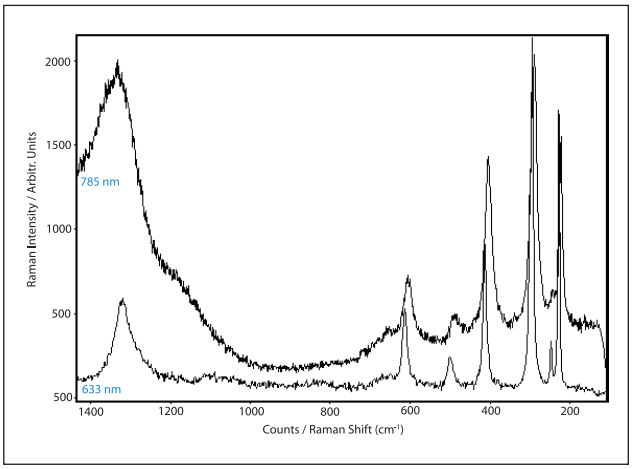

Figure 3. Overlaid spectra displaying the difference in spectral quality between 785 and 633 nm laser excitation.

This systematic method development was carried out using both the 633 and the 785 nm laser with the results reported in Table 2. After comparison, it was decided that the 633 nm laser offered superior results with sharper and better defined peaks (Figure 3), and it is this laser setting that was utilised in the remaining work.

All the spectra collected were taken using the 20× objective lens giving us an analytical area of 5 µm in diameter. The collected spectra were recorded from the surface of the tephra glass shards, from the Hekla eruptions of AD 1510 and 1947, thus removing any potential hydrocarbon contamination from the glass slides (supplementary file 2, available online). The spectrometer was controlled using a PC and Renishaw WiRE 2 as control software.

Principal component analysis (PCA) was carried out using the Eigenvector's PLS_toolbox v. 4.11 within MATLAB. In this work, pre-processing was applied as follows: first, a Savitsky–Golay smoothing filter was applied using a five-point smoothing window and a second-order polynomial deconvolution. Second, a standard normal variate (SNV) analysis was applied. Finally, the datasets were mean-centred.

Results

A thorough analytical examination of the Hekla 1510 and Hekla 1947 samples via Raman spectroscopy revealed that it is possible to identify a range of mineral species. A dominant broad peak, within the spectra collected from the 1947 Hekla ash sample, at 667 cm^{-1} has been assigned to the A_1g species of Fe_3O_4, magnetite (Faria and Vena, 1997; Muralha et al., 2011; Shebanova and Lazor, 2003) (Figure 4).

Further spectral features observed in the spectra from the 1947 ash sample are observed at 670, 460, 396, 324, 266 and 215 cm^{-1} (Figure 5). The peak observed at 324 cm^{-1} Eg (Fe–O sym. bend) have been assigned to magnetite. The peak observed at 460 cm^{-1} has been identified as alpha quartz (Krucnra and Hnvrr, 1994). The additional peaks observed at 396 (Fe–O–Fe/–OH sym. str), 324, 266 Eg (Fe–O sym. bend) and 215 cm^{-1} A1g (Fe–O sym. str) have been assigned to haematite (Chourpa et al., 2005; Legodi et al., 2007).**[AQ: 7]**

Raman analysis of the 1510 Hekla samples was found to be more difficult when compared with the 1947 samples because of issues with fluorescence. Fluorescence within Raman spectroscopy can occur for many reasons including sample colour, causing the excitation photon to not provide sufficient energy to the molecule, or contamination possibly caused by hydrocarbons decomposed on the silica glass surface of the tephra grains (Egerton et al., 1974). If the fluorescence is caused by hydrocarbon contamination, it is possible to reduce the fluorescence with heat treatment, although in this work heat treatment was intentionally avoided because of the risk of chemical changes in the iron oxide chemistry of the sample and because of our belief that fluorescence was not caused by hydrocarbon contamination. Hydrocarbon contamination could lead to distinctive Raman-active modes that we did not observe in our spectra. Fluorescence does not change the nature of the Raman spectra because of it being an absorption process. Fluorescence can simply be overcome with a change in laser excitation or post-processing of the spectra.

The spectral features observed in the 1510 samples (Figure 3) appeared at 512 (Fe–OH asym. str), 465 (Fe–OH asym. Str), 280 (Fe–OH sym. bend), 197 (Fe–O sym. str) (Legodi et al., 2007). These peaks have been attributed to goethite. The two peaks located at 156 and 127 cm^{-1} appear to be the E(LO+TOl) mode of SiO_2 quartz stretch (Krucnra and Hnvrr, 1994). Two of the spectra also contained a large, broad peak at 680 cm^{-1} which has been assigned as magnetite. The peaks observed at 464 nm have been assigned to quartz V_1, indicative of the mineral coesite (Korsakov et al., 2007).

In this study, pre-processing of the spectra was carried out to reduce inherent noise caused either by instrument or sample variability. The Savitsky–Golay smoothing filter was applied in order to smooth the curves of the spectra and thus reduce the noise (Tsai and Philpot, 1998).**[AQ: 8]** This filter does not distort the overall spectra or the frequency position of the peaks. The SNV was performed which is a normalisation method that uses the spectrum itself for correction. SNV achieves this by first by calculating one mean and one standard deviation value for the entire spectrum. It then subtracts the mean value from each spectral point and then divides by the standard deviation. This has the effect of centring the mid-point of the spectrum at zero and standardising the entire spectrum to its overall variance, thus reducing differences in baseline and peak intensity between spectra.

Discussion

Analysis of small tephra shards and cryptotephras with Raman spectroscopy provides a considerable analytical challenge from a spectroscopic point of view. This is because of the fact that volcanic ashes are polyphase (containing both glasses and minerals). Minerals within the volcanic glass exist as phenocrysts and microlites (<0.3 mm), although in this study only the microlites were analysed. Volcanic ashes are

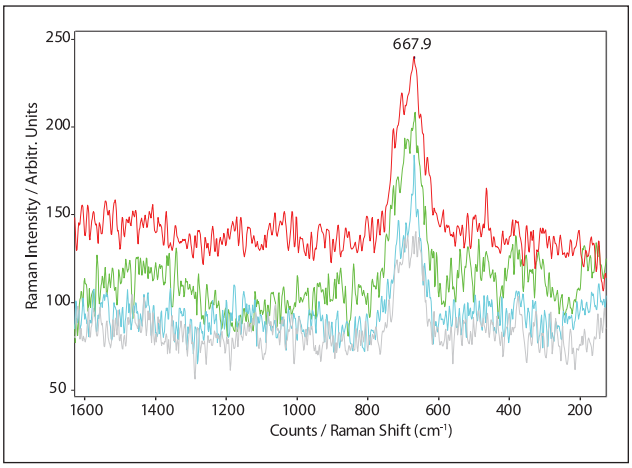

Figure 4. These spectra demonstrate the broad peak at 677 cm^{-1} relating to magnetite from the 1947 tephra. Each of the spectra was collected from a different location on the sample surface.

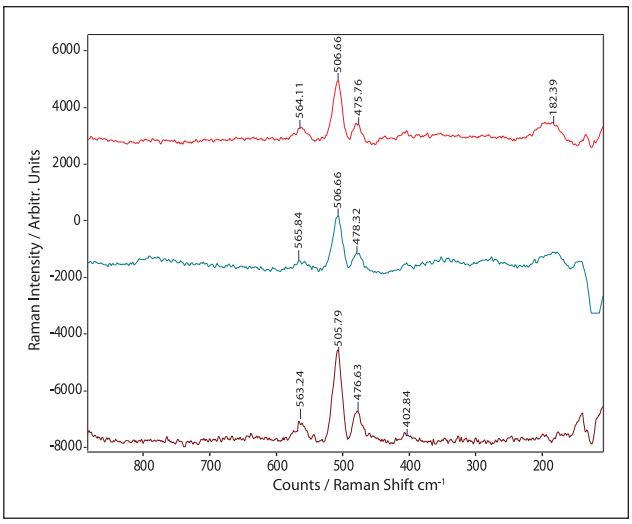

Figure 5. The majority of the spectral features observed in the 1947 sample have been attributed to magnetite (see Figure 2). This figure displays further spectral features observed in sampling sites from the 1947 tephras.

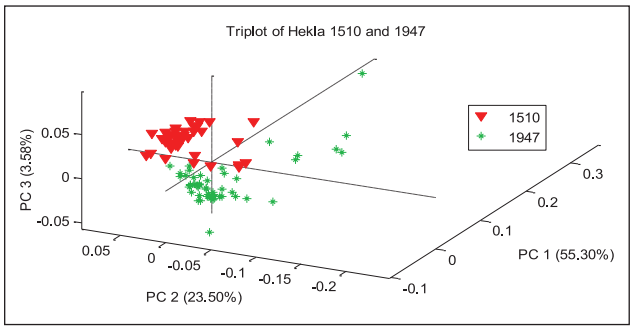

Figure 6. Principal component analysis plot of PC 1 versus PC2 versus PC4. [AQ: 13]

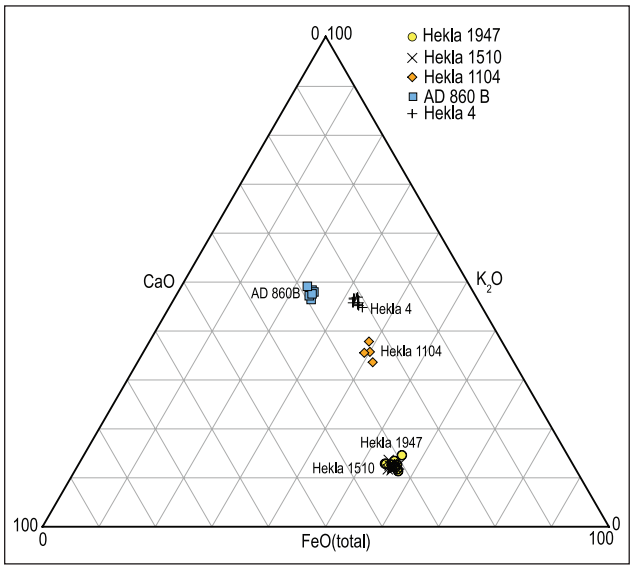

Figure 7. Triplot of 1947 versus 1510 Hekla samples (Ireland) using EPMA along with other recent tephras commonly found in Ireland (after Swindles et al., 2010).

complex and variable in composition (even within a single eruption) and are therefore difficult to analyse (Barletta, 2012).

The newly collected data present some challenges. In the case of heterogeneous samples, the area of the sample illuminated by the laser spot may not be characteristic of the entire sample (White, 2009). In order to resolve this issue, a large amount of data needs to be collected from the sample to obtain a representative sample. Further challenges of laser Raman spectroscopy for mineral identification are laser-induced sample alteration and fluorescence. Although laser Raman spectroscopy is a non-destructive technique, samples can undergo localised heating and oxidation if the laser power is too high (what is considered 'high' laser power depends on the individual sample). Considering our analytical area of 5 µm and power at source of 50 mW, the sample was subjected to a power of 4×10^8 W/cm^2. In this study, the parameter settings of the Raman spectrometer were carefully and systematically designed in order to prevent the sample from overheating which could lead to chemical alteration. This was carefully monitored with the spectra collection on pure iron oxide standards. This presented us with the need for a spectral 'trade-off'. To maintain sample integrity, the signal-to-noise ratio was sacrificed resulting in the need for multiple sample measurements and chemometric analysis (SNV processing) to amplify the differences between spectral datasets. PCA was applied here to identify groups within the data while removing any contribution from background noise.

The spectra were split into two datasets, one set for the 1510 data and one for the 1947 data. After pre-processing, PCA was carried out on the data. This resulted in a number of scores (principal components, PCs) and loadings (spectral variables). The early scores were then plotted against each other to form a three-dimensional score plot with related samples clustering together.

In Figure 6, three PC axes were used and accounted for 98% of the variables within the data. As one can observe in Figure 7, the combined and processed datasets largely split into two data clusters – one representing the 1947 and the other 1510. [AQ: 9] In general, the data relating to the 1947 tephra sit on the left hand side of the axis, while the data from 1510 sit on the right, although there is some overlap. Four of the spectra obtained from the 1510 dataset fall in the main cluster of data from the 1947 data. This cross-over of data can be observed in the individual spectra and has been associated with the presence of small amounts of magnetite within the 1510 data. The data collected through Raman spectroscopy (Figures 4, 5 and 8) offer better discrimination when compared with the data collected through EPMA alone (Figure 1). However, at this time, EPMA data are still required to identify the source volcano.

One further interesting variation observed between the two samples was in the SiO_2 mineralogy observed in the Raman spectra. The Raman spectra obtained from the 1947 sample show traces of α-quartz, as indicated by the peaks at 460 cm^{-1}.

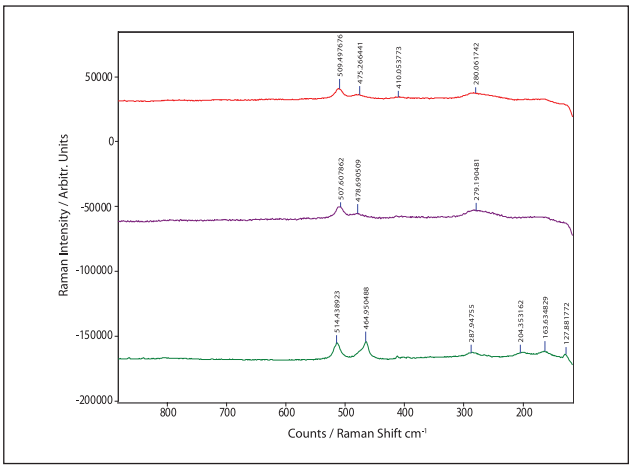

Figure 8. Spectral peaks observed in the sampling sites of the tephra from the Hekla eruption of 1510.

This mineralogy was not unexpected because of the high silica content of the samples shown in previously recorded EPMA data. However, this mineralogy is not observed in the Raman spectra of the 1510 sample, where coesite (Chopin, 1984), a commonly found mineral in rhyolite eruptions (Borisova et al., 2014), was observed instead. The presence of these mineral polymorphs provides further data to support the proposed Hekla 1947 and Hekla 1510 sample discrimination.

Goethite, Haematite and Magnetite were identified through the Raman spectra of both the tephra samples from the Hekla 1947 and Hekla 1510 eruptions. It is well documented that Goethite and Magnetite can convert to Haematite through heating to approximately 250°c. While we cannot comment on these conversions having occurred in nature, we are certain that such conversions were not caused through the experimental procedure and thus are still useful in the separation of the tephras from the Hekla eruptions of AD 1510 and 1947.

Conclusion

Raman spectroscopy has a role to play in the analysis of tephra samples, especially when electron microprobe methods do not provide the level of discrimination required. In this study, we demonstrate that Raman spectroscopy can be used for mineral species identification in tephra enabling the differentiation of glasses with similar chemical composition via the presence of various magmatic crystals contained within the glass. For example, current methods in tephra analysis have hitherto been unable to provide any discrimination between the tephras from the Hekla eruptions of AD 1510 and 1947. Here, we show that Raman spectroscopy can differentiate between these tephras, primarily through the identification of the species forming their iron oxide content, and second, through the presence of their different SiO_2 polymorphs. This Raman method is not designed to be a replacement for current chemical analysis, rather as an additional technique to aid discrimination between compositionally similar tephras. PCA proves to be a good tool for separation of the tephras based on data from Raman spectroscopy; however, a large amount of data is needed for an effective analysis.

Funding

The author(s) received no financial support for the research, authorship, and/or publication of this article.

References

Chopin C (1984) Coesite and pure pyrope in high-grade blueschists of the Western Alps: A first record and some consequences. *Contributions to Mineralogy and Petrology* 86(2): 107–118.

Barletta RE (2012) Raman analysis of blue ice tephra: An approach to tephrachronological dating of ice cores. *Antarctic Science* 24(2): 202–208. DOI: 10.1017/S0954102011000885.

Borisova AY, Toutain J, Dubessy J et al. (2014) RESEARCH ARTICLE H_2O–CO_2–S fluid triggering the 1991 Mount Pinatubo climactic eruption (Philippines). *Bulletin of Volcanology* 76: 800. DOI: 10.1007/s00445-014-0800-3.

Di Carlo I, Rotolo SG, Scaillet B et al. (2010) Phase equilibrium constraints on pre-eruptive conditions of recent felsic explosive volcanism at Pantelleria Island, Italy. *Journal of Petrology* 51(11): 2245–2276. DOI: 10.1093/petrology/egq055.**[AQ: 10]**

Edwards H, Munshi T, Scowen I et al. (2011) Development of oxidative sample preparation for the analysis of forensic soil samples with near-IR Raman spectroscopy. *Journal of Raman Spectroscopy*. Epub ahead of print 2 August. DOI: 10.1002/jrs.3031.

Egerton TA, Hardin AH, Kozirovski Y et al. (1974) Reduction of fluorescence from high-area oxides of the silica, types and Raman spectra for a series of molecules adsorbed on these surfaces. *Journal of Catalysis* 32: 343–361.

Faria DLAD and Vena S (1997) Raman microspectroscopy of some iron oxides and oxyhydroxides. *Journal of Raman Spectroscopy* 28: 873–878.

Haflidason H, Eiriksson J and Kreveld SV (2000) The tephrochronology of Iceland and the North Atlantic region during the Middle and Late Quaternary: A review. *Journal of Quaternary Science* 15(1): 3–22. DOI: 10.1002/(SICI)1099-1417(200001)15:1<3::AID-JQS530>3.0.CO;2-W.

Hall VA and Pilcher JR (2002) Late-Quaternary Icelandic tephras in Ireland and Great Britain: Detection, characterization and usefulness. *The Holocene* 2: 223–230.

Korsakov AV, Hutsebaut D, Theunissen K et al. (2007) Raman mapping of coesite inclusions in garnet from the Kokchetav Massif (Northern Kazakhstan). *Spectrochimica Acta Part A: Molecular and Biomolecular Spectroscopy* 68(4): 1046–1052. DOI: 10.1016/j.saa.2007.04.005.

Krucnra J and Hnvrr J (1994) Raman spectroscopic study of microcrystalline silica. *American Mineralogist* 79: 269–273.**[AQ: 11]**

Larsen G, Dugmore A and Newton A (1999) Geochemistry of historical-age silicic tephras in Iceland. *The Holocene* 9(4): 463–471. DOI: 10.1191/095968399669624108.

Legodi MA, Waal DD and Africa S (2007) The preparation of magnetite, goethite, hematite and maghemite of pigment quality from mill scale iron waste. *Dyes and Pigments* 74: 161–168.

Muralha VSF, Rehren T and Clark RJH (2011) Characterization of an iron smelting slag from Zimbabwe by Raman microscopy and electron beam analysis. *Journal of Raman Spectroscopy* 42(12): 2077–2084. DOI: 10.1002/jrs.2961.

Shebanova ON and Lazor P (2003) Raman spectroscopic study of magnetite ($FeFe_2O_4$): A new assignment for the vibrational spectrum. *Journal of Solid State Chemistry* 174(2): 424–430. DOI: 10.1016/S0022-4596(03)00294-9.

Sverrisdottir G (2007) Hybrid magma generation preceding Plinian silicic eruptions at Hekla, Iceland: Evidence from mineralogy and chemistry of two zoned deposits. *Geological Magazine* 144: 643–659. DOI: 10.1017/S0016756807003470.

Swindles GT, Vleeschouwer FD and Plunkett G (2010) Dating peat profiles using tephra: Stratigraphy, geochemistry and chronology. *Mires and Peat* 7: 1–9.

Thordarson T and Larsen G (2007) Volcanism in Iceland in historical time: Volcano types, eruption styles and eruptive history. *Journal of Geodynamics* 43: 118–152. DOI: 10.1016/j.jog.2006.09.005.

Tsai F and Philpot W (1998) Derivative analysis of hyperspectral data. *Remote Sensing of Environment* 66: 41–51.**[AQ: 12]**

White SN (2009) Laser Raman spectroscopy as a technique for identification of seafloor hydrothermal and cold seep minerals. *Chemical Geology* 259(3–4): 240–252. DOI: 10.1016/j.chemgeo.2008.11.008.